Computer simulation of the interplay between fractal structures and surrounding heterogeneous multifractal distributions. Applications

Miguel Angel Martín , Miguel Reyes , Francisco Javier Taguas

Abstract

In a large number of physical, biological and environmental processes interfaces with high irregular geometry appear separating media (phases) in which the heterogeneity of constituents is present. In this work the quantification of the interplay between irregular structures and surrounding heterogeneous distributions in the plane is made

For a geometric set $A \subset \mathbb{R}^2$ and a mass distribution (measure) μ supported in $S \subset \mathbb{R}^2$, being $A \subset S$, the mass $\mu(A(\varepsilon))$ gives account of the interplay between the geometric structure and the surrounding distribution. A computation method is developed for the estimation and corresponding scaling analysis of $\mu(A(\varepsilon))$, being A a fractal plane set of Minkowski dimension D and μ a multifractal measure produced by random multiplicative cascades. The method is applied to natural and mathematical fractal structures in order to study the influence of both, the irregularity of the geometric structure and the heterogeneity of the distribution, in the scaling of $\mu(A(\varepsilon))$. Applications to the analysis and modeling of interplay of phases in environmental scenarios are given.

Keywords: Fractals; Multifractals; Phases interplay; Fractal dimension; Entropy dimension

1. Introduction

In a large number of scenarios of different scientific fields, objects or regions with irregular borders appear surrounded by phases or media in which a high variability in the concentration of some constituents is a main ingredient. Such is the case of diffusion fronts in chemical reactions [9], wetting fronts in unsaturated soil and porous media [4,9], percolation boundaries [9], river basins [20], tumor growth [1], etc. The mass of such constituents near the border should influence the interplay between phases and thus its estimation becomes imperative. This ubiquitous situation where an irregular geometric structure appears surrounded by a highly heterogeneous distribution suggests it should be modelized and handled by Fractal Geometry tools. Above stimulating objective motivated this research.

After Mandelbrot [16], fractals have been widely used to quantify geometric irregularity in nature. Multifractality, a concept coming from the seminal ideas given in Mandelbrot [15], much more subtle and less popular indeed, has also been used to address heterogeneity. Thus, fractals and multifractals, have proven useful in describing and parameterizing the irregularity of shape via the fractal dimension and the complexity of spatial distributions via the multifractal spectrum, respectively. However, the use of both together to address the picture drawn above has only been addressed recently [18].

Let $A \subset \mathbb{R}^2$ be a fractal set and μ a mass distribution (measure) supported in $S \subset \mathbb{R}^2$ being $A \subset S$. However the amount of measure $\mu(A(\varepsilon))$ surrounding A within an "small neighborhood" $A(\varepsilon) = \{x \in S : \mathrm{dist}(A, x) < \varepsilon\}$ may be positive and, in such case, its relative amount respect to ε gives account of the geometric–measure interplay between both, the set A and the distribution μ.

For uniform measures the quantity $\mu(A(\varepsilon))$ is directly related with the geometric size of $A(\varepsilon)$, and consequently with the fractal dimension of A. For highly heterogeneous distributions however, as is the case of multifractal measures, where the mass concentration (local dimension) varies widely, the estimation should depend on parameters related to the distribution as well. Thus, which heterogeneity parameters of the distribution should be used and how can the parameters used help evaluate the mass–geometry interplay are questions of great interest that need to be answered by means of a precise mathematical treatment.

In Martín and Reyes [18] some asymptotic properties of the mass $\mu(A(\varepsilon))$ including the fractal dimension of the interface and the fractal dimension of the set where the mass of a surrounding multifractal distribution is concentrated, were obtained. However such set is not, in general, a closed set becoming somewhat intangible for the practical estimation of the measure. As a result, the effective estimation will require an adequate computer estimation method. This paper aims to present an interdisciplinary approach for the study of these kinds of problems.

The paper is organized as follows.

First, preliminary theoretical concepts an tools are presented in an accessible way for possible readers interested in the problem though not familiar with Fractal Geometry.

Second, the computation of the mass in different neighborhoods $\mu(A(\varepsilon))$ of the interface is implemented and its scaling behavior studied. This is first done for images of real river networks and later for proper fractal plane sets. The analysis of results allows one to study the influence of both, the irregularity of the geometric structure and the heterogeneity of the distribution, in the scaling of $\mu(A(\varepsilon))$.

Finally several applications for the analysis and modeling of fractal river networks structures and interplay between phases in granular and porous media are suggested.

2. Preliminary concepts

2.1. *Fractal sets and dimensions*

Mathematically speaking irregular fractal structures appear as sets of the Euclidean n-space $\mathbb{R}^n$ with intermediate size between smooth curves and surfaces, that is, sets of non integer Hausdorff dimension.

For $0 \le s \le n$, the s-dimensional Hausdorff measure of a set $A \subset \mathbb{R}^n$ is

$$H^s(A) = \lim_{\delta \downarrow 0} \inf \left\{ \sum_{i=1}^{\infty} d(S_i)^s \;:\; E \subset \bigcup_{i=1}^{\infty} S_i,\ d(S_i) \le \delta \right\}.$$

In particular, the Hausdorff measure H^n is a constant multiple of the Lebesgue measure $\mathcal{L}^n$ (length, area, ...).

The Hausdorff dimension of a set $A \subset \mathbb{R}^n$ is defined by

$$\dim_H A = \inf \{ s \;:\; H^s(A) = 0 \} = \sup \{ s \;:\; H^s(A) = \infty \}$$

and indicates the level at which the measure of the set should be evaluated.

The somehow abstract concept of Hausdorff measure may be replaced by the Minkowski content which is better understood and numerically estimated.

Recall that for $0 < \varepsilon < \infty$ the closed ε-neighborhood of A is

$$A(\varepsilon) = \{ x \in \mathbb{R}^n \;:\; d(x, A) \le \varepsilon \}.$$

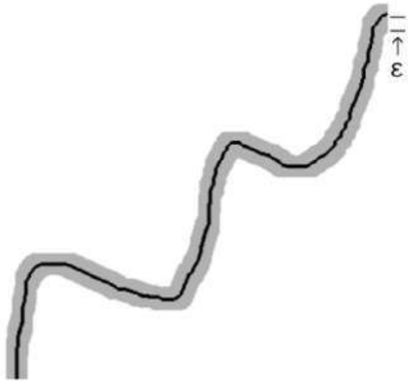

Fig. 1. Minkowski sausage.

The s-dimensional Minkowski content of A is defined by

$$\mathcal{M}^s(A) = \lim_{\varepsilon \to 0} \frac{\mathcal{L}^n(A(\varepsilon))}{(2\varepsilon)^{s-n}}.$$

For nice sets $\mathcal{M}^s(A)$ is a constant multiple of $H^s(A)$ and Hausdorff and Minkowski dimensions agree. Here the term fractal dimension will be used for them without distinction (see [10]).

If $n = 2$, $A(\varepsilon)$ is the Minkowski sausage (Fig. 1).

The fractal dimension of natural structures (river networks, fracture surfaces, ...) is commonly estimated by the well-known box-counting method (see [2,9] or [20] for instance).

Very often irregular geometric structures appearing in different scenarios are modelized by mean of iterated function systems (IFS). Next we present the basic facts about IFS theory (see [7] and [8] for further details).

An iterated function system consists of a finite family of functions $\varphi_i : \mathbb{R}^n \longrightarrow \mathbb{R}^n$, $1 \le i \le m$, where $m \ge 2$ verifying

$$|\varphi_i(x) - \varphi_i(y)| \le r_i |x - y| , \quad \text{for all } x, y \in \mathbb{R}^n$$

with $r_i < 1$, $1 \le i \le m$. An IFS determines a unique nonempty compact set A satisfying

$$A = \bigcup_{i=1}^{m} \varphi_i(A)$$

called the attractor of the IFS.

It can be shown that the set A has Hausdorff and Minkowski dimensions equal to D, being now D the number verifying:

$$\sum_{i=1}^{m} r_i^D = 1.$$

2.2. *Multifractal measures*

Multifractal measures are the mathematical models of high heterogeneous mass distributions (Fig. 2). An example of multifractal measures are the, so called, self-similar measures. Intuitively means that at any region of the support the structure of the distribution resembles the structure of the whole one.

This high complex measures are also easy to obtain by simple iterative process called multiplicative cascades as we shall see later. Roughly speaking, a cascade is a process which fragments a given set (the size interval in this case) into increasingly smaller pieces according to a certain rule and simultaneously divides the distribution of the set according to some (possibly random) mass fragmentation rule. The process defines in the limit a mass distribution that is multifractal.

Fig. 2. Multifractal measure.

Given a finite measure μ on $\mathbb{R}^n$, the local dimension (or local Hölder exponent) of μ at $x \in \mathbb{R}^n$ is given by

$$\dim_{loc} \mu(x) = \lim_{r \downarrow 0} \frac{\log \mu\,(B(x,r))}{\log r}$$

if this limit exists, where $B(a,r)$ denotes the closed ball

$$B(a,r) = \left\{x \in \mathbb{R}^n \;:\; |x-a| \leq r\right\}$$

for $a \in \mathbb{R}^n$ and $0 < r < \infty$. If E is the support of a finite measure μ, for each α the α-layer of μ is the set

$$E_\alpha = \{x \;:\; \dim_{loc} \mu(x) = \alpha\}\,.$$

This set grouping together points with the same concentration of mass for genuine multifractal measures is typically spread along the support of the measure.

The Hölder exponents for self-similar distributions typically span the entire interval between two extreme values α_{min} and α_{max} (see Evertsz and Mandelbrot [6] or Falconer [8], for further details):

$$E = \bigcup_{\alpha_{min} \leq \alpha \leq \alpha_{max}} E_\alpha$$

may be seen as a suggestive representation of heterogeneity as the superposition of homogeneities of different degree.

If $f(\alpha) = \dim_H E_\alpha$ is a continuous function for $\alpha \in [\alpha_{min}, \alpha_{max}]$, μ is said to be multifractal measure and the function $f(\alpha)$ is called the multifractal Hausdorff spectrum or singularity spectrum of the measure μ. See [8] for further details. The function $f(\alpha)$ is parabolically shaped attaining it maximum at the point α_0 being (see Fig. 3)

$$f(\alpha_0) = D_0$$

where D_0 is the Hausdorff dimension of E (the support of the measure μ).

Another important property is that there is $\alpha = \alpha_1$ such that $f(\alpha_1) = \alpha_1$. It can be shown that $D_1 = \alpha_1$ is the Hausdorff dimension of a set that concentrates the whole measure.

The exponent α_0 works as the mean Hölder exponent and the number D_1 is the entropy dimension (see [6]).

The multifractal spectrum may be calculated by the method of moments (see [6] and [9]). However, for experimental measures the direct method presented in [5] has been widely used (see [3] or [17] for instance). Both, D_0 and D_1, are particular cases of the Renyi or generalized dimensions D_q (see [6] and [9]).

3. Computation and scaling analysis of the interplay

A computational method to compute the interplay between irregular/fractal structures (natural and mathematical models) and high heterogeneous distribution is implemented.

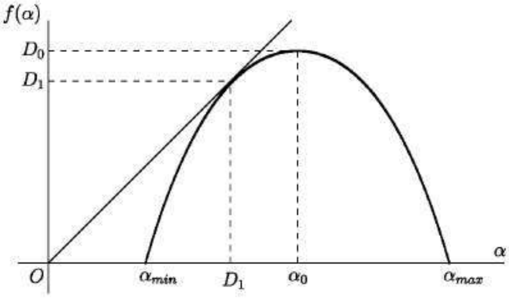

Fig. 3. Multifractal singularity spectrum $f(\alpha)$.

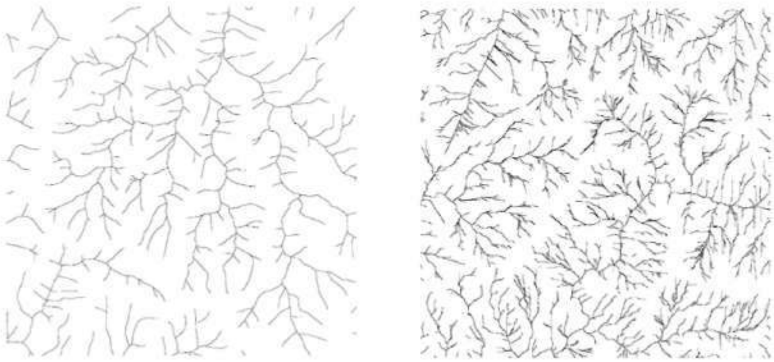

Fig. 4. River networks.

Heterogeneous distributions here used are produced by random cascades processes. Here different cascades are used framed in the general scheme described next.

Let $S \subset \mathbb{R}^2$ be the unit square. Consider the unit mass uniformly spread on S. The square S is divided into four subsquares R_i, $1 \leq i \leq 4$, of side length $1/2$. A mass p_i is supposed uniformly distributed on each R_i, being $\sum_{i=1}^{4} p_1 = 1$. Let φ_i be the linear transformation that transform S into R_i for $1 \leq i \leq 4$. These four transformations are applied first to the square S, and then to any of the resulting squares R_i ("subsquares") following the branching process ad infinitum.

One square of the kth stage of the multiplicative cascade that results from the iterative application of a certain sequence of linear transformations is denoted by $R_{k,j}$. The mass, which is supposed to be uniformly spread in a "son" (subsquare) $R_{k+1,i} = \varphi_i(R_{k,j})$, is given by

$$\mu(R_{k+1,i}) = \mu(R_{k,j})V$$

where V is a random variable that follows a normal distribution of mean p_i, and $\mu(R_{k,j})$ is the mass of the square $R_{k,j}$. At the limit, the process defines a statistically self-similar mass distribution supported on S (see [7] and [8]).

3.1. Natural irregular structures/random cascade heterogeneities

Two real river networks 2-D image A are used as irregular and hypothetic fractal structures (Fig. 4).

Different random multiplicative cascades (different choices for the values of $\{p_i \,:\, 1 \leq i \leq 4\}$) are used to simulate heterogeneous distributions with support in a square S where A is embedded (see Fig. 5).

Let us consider a collection of 4^k ε-boxes R_i of side length $\varepsilon = 2^{-k}$, from $k = 1$ to $k = 10$. At each step, the family $\mathcal{F}$ formed by the subsquares of side $\varepsilon = 2^{-k}$ which meet de set A are selected. Then, the mass accumulated by the $R_i \in \mathcal{F}$ is evaluated and considered as an estimation of $\mu(A(\varepsilon))$ for $\varepsilon = 2^{-k}$:

$$\mu(A(\varepsilon)) \simeq \sum_{R_i \in \mathcal{F}} \mu(R_i).$$

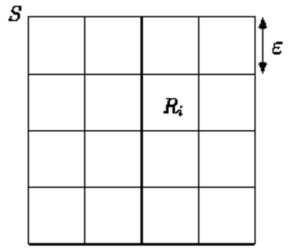

Fig. 5. Dyadic mesh.

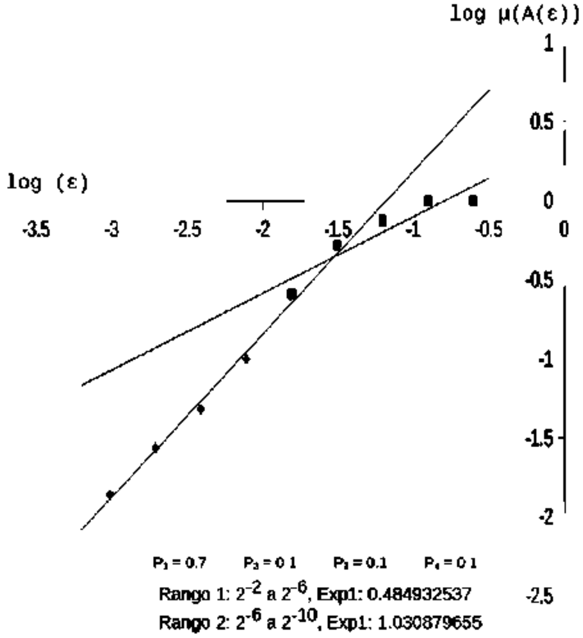

Fig. 6. $\log \mu(A(\varepsilon))$ versus $\log \varepsilon$.

Table 1
Scaling exponent and respective scaling range for river networks 1 and 2.

	Estimated fract dimension	R^2	Scaling range	Scaling exponent	R^2
Network 1	1.29183271	0.97919842	2^{-2}–2^{-6}	0.48493254	0.87284763
			2^{-7}–2^{-10}	0.93967233	0.99781721
Network 2	1.46081451	0.98266654	2^{-2}–2^{-6}	0.12877972	0.69527128
			2^{-7}–2^{-10}	1.05445564	0.99975506

Fig. 6 shows the plot of $\log \mu(A(\varepsilon))$ versus $\log \varepsilon$ for a given cascade. Two different behaviors are detected. One of them in the range 2^{-2}–2^{-6} and the other in the range 2^{-6}–2^{-10}. Table 1 summarizes results which are similar for the different cascades used.

Results seems to indicate that the scaling exponent is influenced by two different sources, one coming from the irregularity of the fractal structure and the other coming from the heterogeneity developed in the cascade. While in the range 2^{-2}–2^{-6} both factors are present, in the range 2^{-6}–2^{-10} only the heterogeneity factor affects the scaling: in the range 2^{-6}–2^{-10} the river networks do not behave as proper fractals.

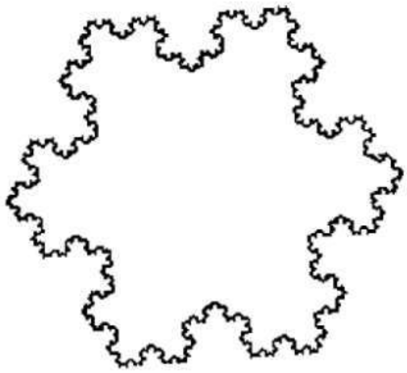

Fig. 7. The Koch island.

Table 2
Scaling exponent and respective scaling range for Koch island and a line.

	Scaling range	Scaling exponent	R^2
Koch island	2^{-2}–2^{-10}	0.74859318	0.99870345
Line	2^{-2}–2^{-10}	1	1

Table 3
Results for the Koch island using different multiplicative cascades.

p_1-p_2-p_3-p_4	Entropy dimension	Scaling exponent	Mean holder exponent
0.3-0.2-0.3-0.2	1.97095059	0.75858164	2.029
0.4-0.2-0.3-0.1	1.84643934	0.79527157	2.176
0.5-0.3-0.1-0.1	1.6854753	0.8117548	2.345
0.6-0.1-0.2-0.1	1.57095059	0.8705677	2.426
0.7-0.1-0.1-0.1	1.35691486	0.89752141	2.62

It should be interesting taking into account this result in the new hydropedology discipline which aims a bridging between traditional pedology, soil physic and hydrology to enhance integrated studies of soil–water relationships across spatial and temporal scales (see H. Lin [14]).

Above result might be useful to facilitate the bridging of data between soil survey databases and soil hydraulic information needed in simulation model to study water quality, landscape processes, nutrient cycling or contaminant fate.

3.2. Fractal set/multiplicative cascade

A proper fractal set A (Koch island) is now considered embedded in the support S (Fig. 7).

Mathematically, the Koch island may be encoded by using IFS (see Peitgen [19]) and it has fractal (Hausdorff and Minkowski) dimension $\log 4/\log 3$. As in previous subsection different multiplicative cascades have been used for the respective distributions, and their respective entropy dimension and mean Hölder exponent using formulas given in Falconer [8].

Considering two choices for the set A, the Koch island and a line, respectively, Table 2 shows the results for the case $p_1 = 1/4$, $1 \leq i \leq 4$, which serves as a paradigm for non singular measures, that is, measures in which the mass concentration is constant. This is the case of classical probability density distributions which have such property as a consequence of the Lebesgue density theorem. For these distributions it can be theoretically argued what the results show: the scaling exponent of $\mu(A(\varepsilon))$ is $2 - D$, being D the fractal (Minkowski) dimension of the fractal structure.

In the singular (multifractal) case, which is the focus of this study, thing dramatically change. Table 3 shows the results for the Koch island and different cascades.

Table 4
Results showing cases with the same entropy dimension and Hölder exponent respectively, but with different scaling exponent.

p_1-p_2-p_3-p_4	Entropy dimension	Scaling exponent	Mean holder exponent
0.4-0.1-0.3-0.2	1.84662335	0.78768145	2.176
0.4-0.1-0.2-0.3	1.84662335	0.74132782	2.176
0.4-0.3-0.2-0.1	1.84662335	0.7766776	2.176
0.4-0.3-0.1-0.2	1.84662335	0.76528888	2.176
0.4-0.2-0.3-0.1	1.84662335	0.79527157	2.176
0.4-0.2-0.1-0.3	1.84662335	0.7376494	2.176

The high R^2 values and the wide range of scaling show an excellent fitting that support the robustness of the scaling.

The entropy dimension, which gives an evaluation of the fractal dimension where the mass is concentrated, statistically correlates with the final scaling exponent of $\mu(A(\varepsilon))$. Also the mean Hölder exponent α_0 correlates. However it seems that no clear quantitative relation may be established between the scaling exponent of $\mu(A(\varepsilon))$, the dimension of the fractal structure and the entropy dimension.

On the other hand results show that distributions with the same entropy dimension and average Hölder exponent α_0 may give different scaling exponents of $\mu(A(\varepsilon))$ (see Table 4).

This may be easily explained by the different geometry/gradient of variability of the corresponding distribution, although they agree in the mentioned attributes. Results support the role of computational studies for any particular case and, on the other hand warn on the risk of the classical use of mean values sampling or using data bases. In spite of this, the multifractal theory shed light on the possible use of the exponents D_1 and α_0 and its difference $\alpha_0 - D_1$ of singularity of spatial variability and its practical implications for prediction purposes. Since both values may be theoretically known for a given modeling or estimated from field data by means of multifractal analysis techniques (Falconer [8]) their interpretation in each scenario may be useful and support the interest of integrating disciplines in the study of these kind of problems.

4. Applications

The above results together with theoretical facts will allow the analysis and modeling of different environmental scenarios with prediction purposes. In the case of real scenarios (dragging of contaminants in river drainage networks for instance) the multifractal analysis of the target distribution (distributions of contaminants if this is the case) provides the multifractal spectrum and, in particular, the values α_0 and D_1. On the other hand the scaling analysis of digitalized data of river networks provides their fractal dimension (Cámara et al. [2]).

A second similar case is the interaction between soil phases at lesser scales, which has a great interest, also can be modeled. According Turcotte's law, the number $N(R)$ of particles larger than a characteristic diameter R follows the scaling rule:

$$N(R) \propto R^{-D}$$

where D is a number known as the "scaling fractal dimension". This fact allow to consider a plane modeling of soil grains by a sequence of disjoint open discs $D_k, k \geq 1$, such that whose boundary has fractal dimension determined by the scaling exponent D (see "cut out sets" in [8]). Denoting by

$$A = Q \setminus \bigcup_{k=1}^{\infty} D_k$$

the void phase, which may eventually be occupied by an heterogeneous distribution of organic matter, nutrients, pollutants.

Finally, the irregularity of wetting front zone where water invades and advances into an originally dry soil has been demonstrated both in the laboratory (Hill and Parlange [12]) and in the field (Starr et al. [21] and Ghodatri and Jury [11]). On the other hand, the high variability and heterogeneity in the distribution of chemicals, nutrients and pollutants, have been parameterized by multifractal analysis (Kravchenko et al. [13]). In this situation one obtains the picture drawn throughout the paper and the ideas and results here given can be applied.

5. Conclusions

In many natural scenarios interfaces with high irregular geometry appear separating media (phases) in which the heterogeneity of constituents is present. The problem of measuring the interplay between an irregular (fractal) geometric structure surrounded by a highly heterogeneous (multifractal) distribution, recently posed, has a great interest under theoretical, computational and practical points of view.

For a geometric set $A \subset \mathbb{R}^2$ and a mass distribution (measure) μ supported in S, being $A \subset S$, the mass $\mu(A(\varepsilon))$ gives account of the interplay between the geometric structure and the surrounding distribution. The computer simulation of $\mu(A(\varepsilon))$ in natural and mathematical structures leads to power scaling rules whose scaling exponent is simultaneously affected by two different sources: the irregularity of the fractal structure and the heterogeneity of the surrounding distribution.

Using natural structures and random multiplicative cascades, the analysis shows the existence of a lower limit of the scaling for natural structures.

When testing mathematical models are used, the study shows different relationships between the mass $\mu(A(\varepsilon))$, the fractal dimension of the structure A, and the entropy dimension and mean Hölder exponent of the surrounding distribution. Since those parameters may be estimated in natural systems, or theoretically known in mathematical structures, the results here obtained may be used in the analysis and modeling of physical and environmental scenarios.

Acknowledgments

Authors wish to acknowledge the valuable help received from Roberto Simal in the implementation of the computer programs. Also the help of F.J. Muñoz is acknowledged.

This research work was partially funded by Spain's Plan Nacional de Investigación Científica, Desarrollo e Innovación Tecnológica (I+D+I) under ref. AGL2011-25175.

References

[1] A. Bru, J.M. Pastor, I. Fernand, I. Bru, S. Melle, C. Berenguer, Super-Rough dynamics on tumor growth, Phys. Rev. Lett. 81 (1998) 4008–4011.
[2] J. Cámara, V. Gómez-Miguel, M.A. Martín, Lithologic control on the scaling properties of the first-order streams of drainage networks: A monofractal analysis, Vadose Zone J. 12 (3) (2013). http://dx.doi.org/10.2136/vzj2012.0205.
[3] F.J. Caniego, M.A. Martín, F. San José, Singularity features of pore-size soil distribution: singularity strength analysis and entropy spectrum, Fractals 9 (3) (2001) 305–316.
[4] W.L. Chang, J.W. Biggar, D.R. Nielsen, Fractal description of wetting front instability in layered soils, Water Resour. Res. 30 (1994) 125–132.
[5] A. Chhabra, R.V. Jensen, Direct determination of the $f(\alpha)$ singularity spectrum, Phys. Rev. Lett. 62 (1989) 1327–1330.
[6] C.J.G. Evertsz, B.B. Mandelbrot, Multifractal measures, Appendix B, in: H.O. Peitgen, et al. (Eds.), Chaos and Fractals, Springer Verlag, New York, 1992, pp. 921–953.
[7] K.J. Falconer, Fractal Geometry, John Wiley & Sons, New York, 1990.
[8] K.J. Falconer, Techniques in Fractal Geometry, John Wiley & Sons, New York, 1997.
[9] J. Feder, Fractals, Plenum Press, New York, 1988.
[10] H. Federer, Geometric Measure Theory, Springer-Verlag, New York, 1969.
[11] M. Ghodatri, W.A. Jury, A field study using dyes to characterize preferential flow of water, Soil Sci. Soc. Am. J. 54 (1990) 1558–1563.
[12] D.E. Hill, J.Y. Parlange, Wetting front instability in layered soils, Soil Sci. Soc. Am. Proc. 36 (1972) 697–702.
[13] A.N. Kravchenko, C.W. Boast, D.G. Bullock, Multifractal analysis of soil spatial variability, Agron. J. 91 (1999) 1033–1041.
[14] H. Lin, Hydropedology: Bridging disciplines, scales and data, Vadose Zone J. 2 (2003) 1–11.
[15] B.B. Mandelbrot, Intermittent turbulence in self-similar cascades: Divergence of high moments and dimension of the carrier, J. Fluid Mech. 62 (1974) 331–358.
[16] B.B. Mandelbrot, The Fractal Geometry of Nature, W.H. Freeman, New York, 1982.
[17] M.A. Martín, E. Montero, Laser diffraction and multifractal analysis for the characterization of soil dry volume-size distributions, Soil Tillage Res. 64 (1-2) (2002) 113–123.
[18] M.A. Martín, M. Reyes, A fractal interaction model for winding paths through complex distributions: Application to soil drainage networks, Pure Appl. Geophys. 165 (2008) 1153–1165.
[19] H.O. Peitgen, H. Jürgens, D. Saupe, Chaos and Fractals, Springer Verlag, New York, 1992.
[20] I. Rodríguez-Iturbe, A. Rinaldo, Fractal River Basins, Chance and Selforganization, Cambridge University Press, Cambridge, 1997.
[21] J.L. Starr, J.Y. Parlange, C.R. Fink, Water and chloride movement through a layered field soil, Soil Sci. Soc. Am. J. 50 (1986) 1384–1390.